This article has been accepted for publication in a future issue of this journal, but has not been fully edited. Content may change prior to final publication. Citation information: DOI 10.1109/TBME.2016.2553131, IEEE Transactions on Biomedical Engineering

# Seizure Prediction using Undulated Global and Local Features

Mohammad Zavid Parvez, *Student Member, IEEE* and Manoranjan Paul, *Senior Member, IEEE*

***Abstract*—In this study a seizure prediction method is proposed based on a patient-specific approach by extracting undulated global and local features of preictal/ ictal and interictal periods of EEG signals. The proposed method consists of feature extraction, classification, and regularization. The undulated global feature is extracted using phase correlation between two consecutive epochs of EEG signals and an undulated local feature is extracted using the fluctuation and deviation of EEG signals within the epoch. These features are further used for classification of preictal/ictal and interictal EEG signals. A regularization technique is applied on the classified outputs for the reduction of false alarms and improvement of the overall *prediction accuracy* (PA). The experimental results confirm that the proposed method provides high PA (i.e. 95.4%) with low false positive per hour using intracranial EEG signals in different brain locations of 21 patients from a benchmark data set. Combining global and local features enables the transition point to be determined between different types of signals with greater accuracy, resulting successful versus unsuccessful prediction of seizure. The theoretical contribution of the study may provide an opportunity for the development of a clinical device to predict forthcoming seizure in real time.**

***Index Terms*— Deviation, Epilepsy, Fluctuation, LS-SVM, Phase Correlation, Seizure**

## I. INTRODUCTION

SEIZURE is a sudden surge of electrical activity of the brain affecting more than 65 million individuals (i.e. 1%) worldwide [1]. Approximately 325 million people experience a seizure within their life time [2]. During seizure, the brain cannot perform normal tasks; therefore, people may restriction and abnormal activity in movement, behavior, awareness, and sensation. Epilepsy is spontaneously recurrent seizures. Seizure causes many injuries such as submersion, burns, accidents, and more seriously, death. However, it is possible to prevent these unwanted situations by timely and correct prediction of epilepsy before the actual seizure onset. *Electroencephalogram* (EEG) is a well-accepted tool for analyzing seizure [3]-[28]. EEG can measure electrical activity of the brain through multiple electrodes placed on the scalp [8].

A significant amount of research of seizure prediction including [23]-[28] has been conducted. Williamson *et al*. [23] proposed a seizure prediction method based on spatiotemporal features. The experimental results provide 85% accuracy with *false positive rate* (FPR) of 0.03/h using 19 patients from a total of 21 patients using the benchmark data set [29]. Chisci *et al*. [24] also proposed a prediction method using an autoregressive model and *support vector machine* (SVM). The *prediction accuracy* (PA) was 100% with FPR of 0.41/h using only 9 patients from the same data set [29]. Mirowski *et al*. [25] proposed another method based on bivariate features such as cross-correlation, nonlinear interdependence, and dynamic entrainment using the data set in [29] where the results provided 71% accuracy with zero FPR using 15 of 21 patients. Park *et al*. [2] proposed a technique using linear features of spectral-power and non-linear classifier considering 18 of 21 patients that provided 94.4% accuracy with FPR of 0.20/h using the data set [29]. Li *et al*. [26] employed the spike rate using a morphological filter and obtained 75.8% PA with FPR of 0.09/h using all 21 patients from the data set [29]. Moghim *et al*. [27] proposed a seizure prediction technique in advance using different statistical features by preictal period relabeling of the EEG signals. They obtained high accuracy (i.e. 96.30%) for prediction between 1 and 6 minutes in advance using the data set [29]. Rasekhi *et al*. [28] proposed a seizure prediction technique based on linear univariate features by providing 73.9% PA with FPR of 0.15/h using another data set.

It is difficult to achieve a good balance by using a prediction algorithm between high PA (100%) with low FPR, using all patients. Moreover, for a given *seizure prediction horizon* (SPH), it is also difficult to achieve prediction performance above the chance level for all patients by a particular method [11]. The non-abruptness phenomena and inconsistency of the signals along with different brain locations, patient-age, patient-sex, and seizure-type are the challenging issues that affect the consistency of performance in terms of advanced PA and

Manuscript submitted for review July 10, 2015.This work was supported in part by the CM3 Machine Learning Research Centre, Charles Sturt University, Australia.

The authors are with CM3, Charles Sturt University, Australia (e-mail: {mparvez; mpaul}@csu.edu.au).

This article has been accepted for publication in a future issue of this journal, but has not been fully edited. Content may change prior to final publication. Citation information: DOI 10.1109/TBME.2016.2553131, IEEE Transactions on Biomedical Engineering

false alarms by the existing methods using all types of patients. Therefore, more research should be conducted within this scope to achieve better accuracy for advanced prediction with low FPR.

When an EEG signal is captured from a patient, it may have different types of periods such as interictal, preictal, and ictal periods, in that order. Thus, for the advanced prediction of an ictal state, the transition between interictal and preictal periods needs to determine, as EEG is a supreme advantage in studying transient neuronal activity [30]. How early a preictal period associated with an ictal period is determined from the interictal period by a technique indicates its advanced prediction performance accuracy. To determine the transition between interictal and preictal periods, an EEG signal needs to be processed by dividing the signal into a number of epochs (i.e. a specified time-window). Sometimes the epoch is not fully aligned with the interictal, preictal, or ictal period i.e. an epoch may have two types of period if an epoch is very large in size. Thus, it is important to extract global features from different epochs and local features within an epoch for correct seizure prediction. Moreover, the features extracted from spatially separated different channels of EEG signals should be incorporated to further improve the PA. In this paper, a novel approach is derived by exploiting spatiotemporal correlation of undulated global and local features within an EEG signal to find the transition of an event occurring during a seizure.

Phase correlation [31] essentially provides relatively shifting information between current signals and reference signals of two correlated signals via Fourier Transformation. Thus, *undulated global feature* (UGF) can be determined using phase correlation. Paul *et al*. [31] demonstrated that the phase correlation is capable of detecting reliable motion between two images or blocks. In a similar fashion, the phase correlation extracting features between two adjacent epochs can capture the relative changes between two epochs of an EEG signal. This can be used to estimate the transition between interictal and preictal/ictal periods. However, sometimes this may not be adequate to identify the transition, if the transition is not aligned with the epochs. To avoid this situation, a local feature is also extracted from the signal fluctuation and deviation from the frequent oscillation within an epoch to achieve better accuracy and significant reduction in false alarms. Xie *et al*. [32] illustrated that fluctuation and deviation are able to identify defects of an image. This inspired us to use customized fluctuation and deviation [32] which can measure the fine changes of a specific epoch. Therefore, a cost function comprised of weighted fluctuation and deviation in each epoch is calculated in a temporal direction to extract the *undulated local feature* (ULF). Since EEG signals are non-stationary signals [33], the *cost function of fluctuation and deviation* (CFD) cannot fully identify the phase-lagging between two epochs alone. Thus, in this paper, both features (i.e. UGF and LGF) are used for advanced prediction of seizure onset with greater PA and low FPR.

The paper is organized as follows: the data formation, the detailed proposed technique, feature extraction, classification, and post-processing are described in Section 2. Definition of SPH and statistical validation is described in section 3, and the detailed experimental results and discussions are explained in Section 4. Section 5 contains the analysis of results, and Section 6 the conclusion.

## II. Proposed Method

The key objective of the paper is to successfully predict seizure with high accuracy in an automated way. A generic diagram of a seizure prediction process is schematized in Fig. 1 with a detailed description of the process diagram presented below. In general, pre-processing, features extraction, classification, regularization (i.e. post-processing) and decision function are all possible steps for predicting seizure from EEG signals. Normally a pre-processing step is applied to remove artifacts from the raw EEG signals using filtering techniques. However, our proposed method is considered with a certain range of artifacts tolerance without a filtering technique being applied. Firstly, different features are extracted using different approaches. These features are then used to classify different types of periods and regularization (i.e. post-processing) is used on classified signals to enable a final decision to be made for predicting seizure. In the proposed method, phase correlation and CFD are used as a feature extraction procedure, with *least square-SVM* (LS-SVM) as a classifier, and windowing regularization as a post-processing step. Our contributions are customization of the existing phase correlation, and cost function of fluctuation and deviation techniques, all are applicable in EEG signals analysis for the feature extraction of EEG signals. An innovative regularization is also proposed to enable a final decision on the type of interictal and preictal/ictal periods.

### *A. Data Formation*

The paper uses the data set recorded at the Epilepsy Centre of the University Hospital of Freiburg, Germany

This article has been accepted for publication in a future issue of this journal, but has not been fully edited. Content may change prior to final publication. Citation information: DOI 10.1109/TBME.2016.2553131, IEEE Transactions on Biomedical Engineering

[29]. The data set is publicly available and the most cited resource in modern seizure detection and prediction approaches [8]-[27][33]-[36] that contains *intracranial EEG* (iEEG) recordings of 21 patients suffering from medically intractable focal epilepsy [34]. The data was obtained by the Neurofile NT digital video EEG system with 128 channels, 256 Hz sampling rate, and 16 bit analogue-to-digital converter. In this data set, the epileptic EEG signals are classified into ictal, preictal, postictal, and interictal periods. The ictal period may persist from a few seconds to 5 minutes. The ictal-records (which is tagged as an ictal file) contains at least 50 minutes of preictal signals preceding each seizure. The data set contains 87 seizures from 21 patients. Altogether, it is 24-25 hours of interictal signals and 2-5 hours of ictal signals with preictal and postictal signals [29]. Therefore, the data set is around 509 hours. For the experiments, we concatenate 60 minutes of interictal signals and 30 minutes of preictal/ictal signals (as 30 minutes preceding a seizure onset) for each seizure of a patient. In this way we consider all seizures for all patients in the data set. There is no clear chronological order between interictal and preictal EEG signals in the Freiburg data set for a patient. The signals are arranged into different numbers of blocks with each block containing approximately 1 hour signals. We organize the signals for interictal and preictal/ictal signals one after another by maintaining continuous signals within interictal and preictal periods individually. It is to be noted that six channels are used to capture EEG signals in each patient. In the experiments, all channels of focal electrodes (i.e. three channels) and extra-focal (i.e. another three channels) electrodes for EEG signals from different brain locations and different patients are considered.

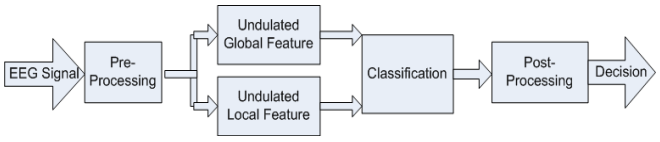


Fig. 1. Generic block diagram of a seizure prediction process.

### *B. Undulated Global Feature (UGF) Extraction*

It is assumed that an EEG signal of a channel captured from a patient contains interictal, preictal, and ictal periods, in that order. To identify a particular signal type (i.e. ictal, interictal, or preictal period) an EEG signal is divided into small epochs or time-windows. Relative change is estimated between the current epoch and the successive epoch using phase correlation. The relative change between successive epochs indicates whether there is any signal-type change from interictal to preictal or ictal to interictal period. Features are extracted from the relative changes among epochs. See a block diagram of the proposed global feature extraction in Fig. 2. The detailed procedure of the feature extraction is described below.

Let $r$ and $c$ be the previous (i.e. reference) and current epoch respectively, containing all values of the specified time-window of the EEG signals. Corresponding transformed signals $R$ and $C$ are determined after applying *Fast Fourier Transformation* (FFT) on the reference and current epochs as follows:

$$R = \varphi(r) \tag{1}$$

$$C = \varphi(c) \tag{2}$$

where $\varphi$ is the FFT function.

A phase correlation $\zeta$ of $r$ and $c$ is then determined using transformed signals by applying inverse FFT and shift FFT (these functions are available in Matlab) as follows:

$$\zeta = \vartheta\left|\varphi^{-1}\left(e^{j(\angle R - \angle C)}\right)\right| \tag{3}$$

where $\vartheta$ is the FFT shift function and $\angle$ indicates the angle or phase. Then the displacement between two epochs is determined as follows:

$$k = \max_{\arg t}(\zeta(t)) - \pi \tag{4}$$

where the middle position of the epoch is considered as $\pi$ and $t$ is any sample position within the epoch.

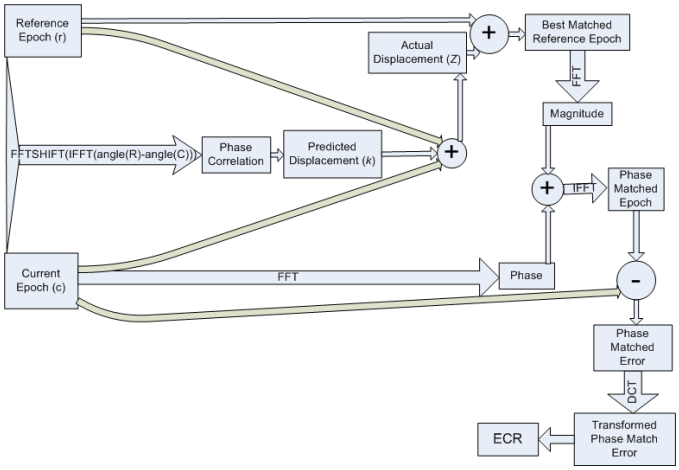


Fig. 2. Extracted global feature by phase correlation.

To find the actual displacement z between two epochs, the minimum *mean square error* (MSE) of the reference epochs against the current epoch is examined from the predicted displacement to the '0' locations where '0' location means the original reference epoch location. In the experiments a 10 second epoch is considered. Thus, an epoch size, $\beta$, is 2560 (=10 × 256)

This article has been accepted for publication in a future issue of this journal, but has not been fully edited. Content may change prior to final publication. Citation information: DOI 10.1109/TBME.2016.2553131, IEEE Transactions on Biomedical Engineering

samples, where the length of the epoch is 10 seconds and the samples per second is 256. To understand locations of the current and reference epochs of a signal, it is assumed that if the current epoch is started at a position of 200th seconds, then the reference epoch is started at 190th seconds. If a given current epoch provides the best-matched reference epoch with a displacement of $k$ = 100 using the phase correlation (see Equation (4)), all reference epochs are needed to be checked from the original reference epoch (i.e. '0' location) to other epochs formed by shifting 1 to 100 samples in the right direction (see bottom epochs in Fig. 3). In this case, some samples of the reference epochs overlap with the current epoch. On the other hand, if $k$ = -100, all reference epochs are needed to be checked from the original reference epoch to other epochs formed by shifting 1 to 100 samples in the left direction (see top reference epochs in Fig. 3). The best-matched reference epoch is calculated as follows:

$$\lambda = r(t + \mathrm{Z}) \tag{5}$$

where $\mathrm{Z} = \arg\min_{i} \left( \frac{1}{\beta} \sum_{i=0}^{\tau} (r(t+i) - c)^2 \right)$.

Actually λ is the Z-position shifted reference epoch which provides minimum difference with the current epoch $c$.

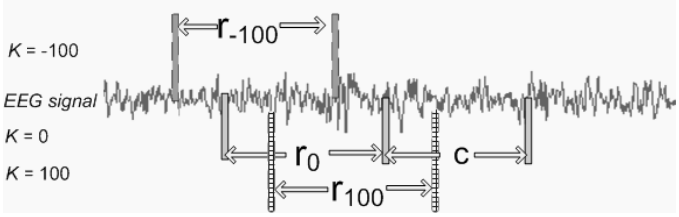


Fig. 3. Visualization of different best-matched epochs for a given current epoch using phase correlation where the reference epochs are calculated from 0 to displacement (i.e. k) positions based on the MSE between the current epoch and the reference epochs of a signal.

The phase-matched reference epoch is calculated as follows, where inverse FFT is applied on the frequency epoch with the phase of the current epoch and the magnitude of the best-matched reference epoch:

$$\psi = \left| \varphi^{-1} \left( |\varphi(\lambda)| e^{j\angle C} \right) \right|. \tag{6}$$

The phase-matched error is calculated between the current and phase-matched reference epochs as follows:

$$\varepsilon = c - \psi. \tag{7}$$

Then *discrete cosine transformation* (DCT) is applied on the phase-matched error in order to calculate the transformed residual as follows:

$$\partial = \phi(\varepsilon) \tag{8}$$

where $\phi$ is the DCT function. DCT is an effective transformation to convert a signal from the time domain to the frequency domain, and to arrange them from low to high frequency coefficients [37]. If the original signal (see Fig. 4.(a)) has less variations, then all energy of the DCT transformed signals is concentrated in the first few coefficients; otherwise, the energy is distributed into all coefficients. This property is exploited to find the energy concentration ratio between low and all frequency coefficients.

Finally, an *energy concentration ratio* (ECR) is calculated by the ratio of total energy from the low frequency coefficients and the entire coefficients of $\partial$ as follows:

$$\Re = \sum_{s=1}^{\lfloor 3\beta/4 \rfloor} \partial^2(s) \Big/ \sum_{t=1}^{\beta} \partial^2(t). \tag{9}$$

The *mean ECR* (MECR) is calculated using all channels of the specific patient as follows (see Fig. 4.(b)):

$$\omega = \frac{1}{N} \sum_{i=1}^{N} \Re_i \tag{10}$$

where $0 < \omega < 1$ and $N$ is the total number of neighboring channels and $\Re_i$ is the ECR of $i^{\text{th}}$ channel.

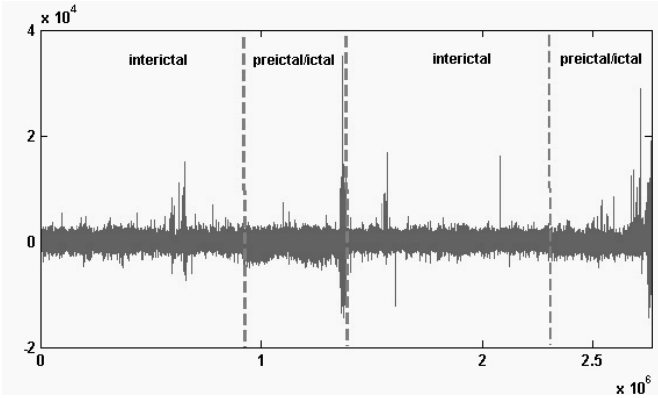


(a) Original EEG signals comprises interictal and preictal/ictal periods.

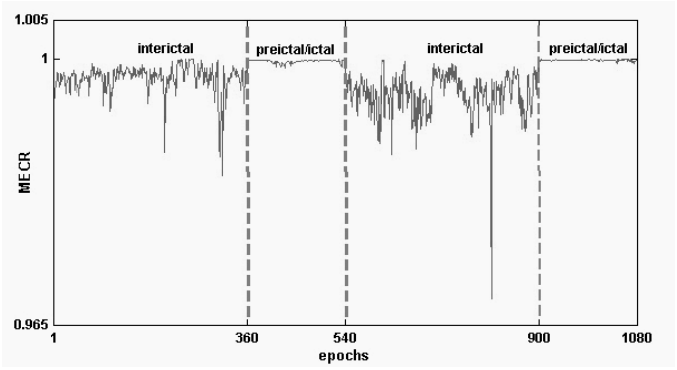


(b) Mean energy concentration ratio i.e. MECR of interictal and preictal/ictal periods using six channels.

Fig. 4. Preictal/ictal and interictal EEG signal from patient 17 and channel 1 where (a) represents the raw EEG signals (b) represents MECR where vertical lines are drawn to separate the interictal periods from preictal/ictal periods.

The MECR is used as an undulated global feature i.e. UGF for the classifier. Fig. 4. (b) shows that the values of MECR for preictal/ictal are relatively higher

This article has been accepted for publication in a future issue of this journal, but has not been fully edited. Content may change prior to final publication. Citation information: DOI 10.1109/TBME.2016.2553131, IEEE Transactions on Biomedical Engineering

compared to that of the interictal signal. This indicates that MECR would be a good feature to classify a preictal/ictal signal from an interictal signal. One can easily find the corresponding time in seconds by multiplying 10, as our epoch size is 10 seconds. As our initial processing unit is an epoch, thus we use an epoch as an x-axis unit in this case.

### *C. Undulated Local Feature (ULF) Extraction*

Using fluctuation and deviation, Xie *et al*. [32] show that local defect merit function quantifies the cost of an image where a pixel of an object is defective or not. Fluctuation of a group of signals or pixel intensities is considered as the changes of overall signals or pixel intensities within the group. Thus it reflects the overall variations from the average trend of the signals or pixel intensities within the group. On the other hand, deviation reflects the variations from the most common trend of the signals or pixel intensities within the group. Inspired by the paper [32], a customized fluctuation and deviation function is used to measure the local relative change of an EEG signal for identifying different types of signals such as interictal and preictal/ictal. The calculation of fluctuation and deviation is performed using a 10 second epoch with 128 samples shifted (the justification of selecting epoch size and shifting size is given in Sections IV.A and IV.B respectively). Unlike the technique in [32], the fluctuation function is refined as follows for the current epoch:

$$f = \sigma(c) - \delta \tag{11}$$

where $\sigma$ is the *standard deviation* function applied on the source (i.e. original) signal of each epoch, and $\delta$ is the general artifacts component of the EEG signal. In the experiments, $\delta = 4$ is used. Unlike the technique in [32], we shifted the epoch by 128 samples (see in Equation (11)) and calculated $f$ for each shifted epoch. Thus, for a given 10-second epoch it has 20 values of $f$. The deviation function of the current epoch is also redefined as follows:

$$d = \frac{1}{\beta}\sum_{x=1}^{\beta}\left|c(t) - \gamma\right| \tag{12}$$

where $\gamma$ is the *mode* of the original signal $c$.

Finally a cost function $\wp$ is calculated for each shifted epoch using weighted fluctuation and deviation as follows (see Fig. 5 (a)):

$$\wp = w_1 \times d^2 + w_2 \times f^2 \tag{13}$$

where $w_1$ and $w_2$ are a weighted value of deviation and fluctuation, respectively. In the experiments, $w_1 = 1/16$ and $w_2 = 1$ are used as suggested in [32].

As 128 samples are shifted for the shifted epoch to calculate the cost function $\wp$ (see Fig. 5(a)), the cost function quantifies 20 values of a 10 seconds epoch. From the current epoch, the *energy of cost functions of the fluctuation and deviation* (ECFD) is calculated as the second feature (see Fig. 5(b)):

$$\Phi = \sum_{l=1}^{n} \wp_l^2 \tag{14}$$

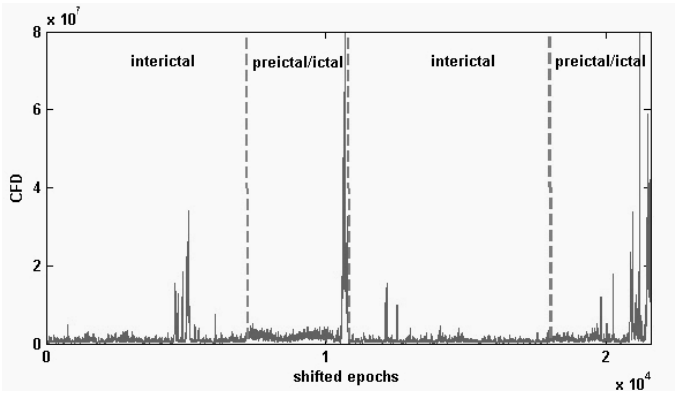


(a) Values after applying cost function of fluctuation and deviation (CFD) on interictal and preictal/ictal periods.

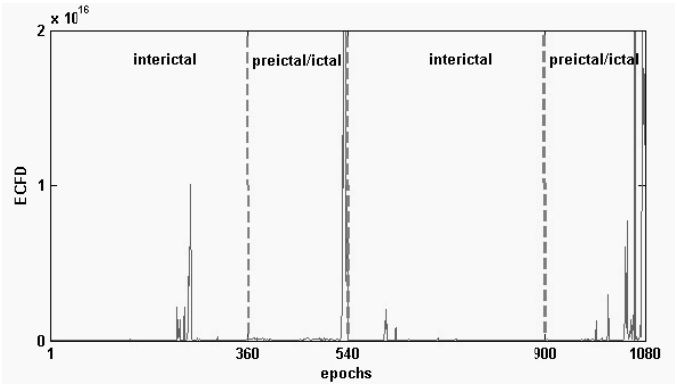


(b) Energy of CFD i.e. ECFD of interictal and preictal/ictal periods using six channels.

Fig. 5. CFD technique applies on preictal/ictal and interictal EEG signal from patient 17 and channel 1 where (a) represents the combined value of CFD and (b) represents energy of CFD value where vertical lines are drawn to separate the interictal periods from preictal/ictal periods.

The detailed process of extracting a local feature is presented in Fig. 6.

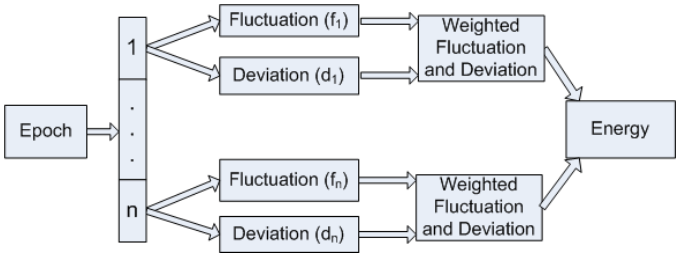


Fig. 6. Extracted local feature using fluctuation and deviation.

This article has been accepted for publication in a future issue of this journal, but has not been fully edited. Content may change prior to final publication. Citation information: DOI 10.1109/TBME.2016.2553131, IEEE Transactions on Biomedical Engineering

*D.Classification*

To classify the preictal/ictal and interictal signals, two features, MECR, $\omega$ and ECFD, $\Phi$ are considered. For classification, a SVM-based classifier is used as the SVM [38] works as one of the best classifiers for the non-stationary signals, such as EEG signals [39][40]. LS-SVM is an extended version of SVM and can minimize the higher computational burden of the constrained optimization programming of SVM [41]. Therefore, LS-SVM [42][43] is used for classification in the experiments. The equation of LS-SVM is defined in [44] as:

$$\Gamma(x) = sign\left[\sum_{m-1}^{N} \alpha_m y_m \Delta(x, x_m) + b\right] \quad (15)$$

where $\Delta(x, x_m)$ is a kernel function, $\alpha_m$ are the Lagrange multipliers [45], $b$ is the bias term, $x_m$ is the training input, and $y_m$ is the training output pairs. Equation (15) is used to find a maximum-margin hyper-plane to classify interictal and preictal/ictal signals.

RBF kernel is used in our experiments as this is one of the most effective kernels for non-stationary EEG signal classification. This function can be defined as:

$$\Delta(x, x_m) = \exp(-\|x - x_m\|^2 / 2\Theta^2) \quad (16)$$

where $\Theta$ controls the width of RBF kernel function. The RBF kernel is a fast and linear algorithm capable of representing complex non-linear mapping. A detailed formulation of LS-SVM can be found in [41][42].

The classifier aims to classify preictal/ictal and interictal EEG signals using a machine learning approach. The selection of the parameters is automated by optimizing a cross-validation based model selection. In the experiments, cross-validation is conducted for tuning the parameters which are then used for testing. To find mapping between a training set and an unseen test set is challenging. LS-SVM is a classifier that learns nonlinear mapping from the training set features $\{x\}_m$=1…$n_T$, where $n_T$ is the number of training features in the patient's state of preictal/ictal period (1) and interictal period (0). To obtain unbiased classification results [46] and to make sure testing data has never been used for training, we follow the same procedure suggested by Park *et al*. [2]. In the experiment, if a patient has $M$ seizures and $N$-hour-long interictal recording, then whole trails of interictal signals are divided into the $M$ subset, where each subset contains $N/M$ hour long interictal recoding with 30 minutes preictal/ictal signals. One interictal and preictal/ictal subset is randomly chosen and reserved for testing and the remaining $M$-1 is used for training. Ten- fold cross validation is performed during training to generate an optimal model of the LS-SVM classifier. 90% of the training set, the whole training set is considered as the $M$-1 subset, is randomly selected to establish the LS-SVM model in the learning processing and the remaining 10% is used to fit the model. Once the model is well-fitted then the model is considered as trained and the reserved subset is evaluated by testing. This process is performed $M$ times and the average classification rate is considered.

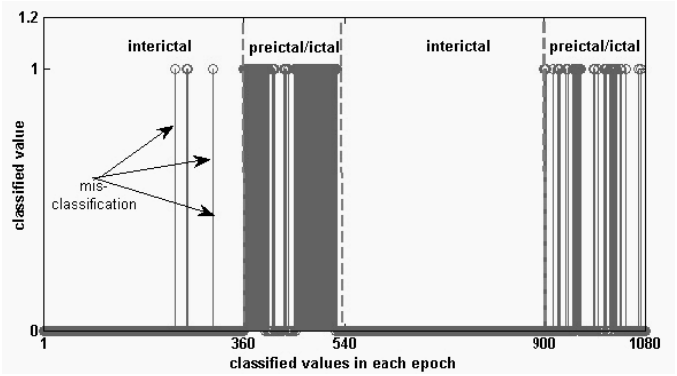


(a) Classified results of each epoch of an interictal and preictal/ictal periods.

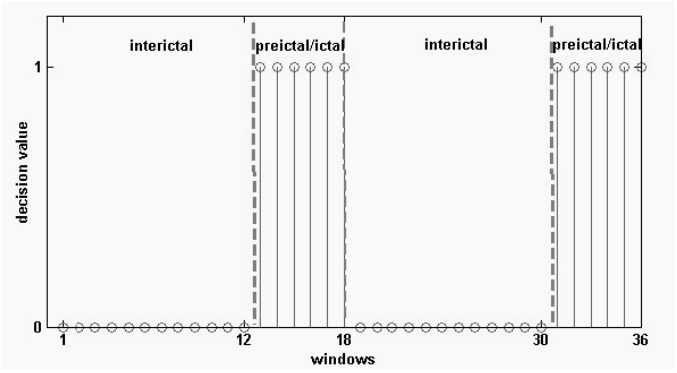


(b) Decision on classified values after windowing of interictal and preictal/ictal periods.

Fig. 7. A demonstration of the classified output after LS-SVM classification and proposed regularization using EEG signals from Patient 17 where (a) represents the classification output using LS-SVM and (b) represents the decision of seizure prediction after regularization.

*E.Post-processing*

Undulated local and global feature extraction techniques inherently attenuate unwanted signals as artifacts with eye blinking, muscle movement, etc. These artifacts may lead to misclassification of preictal/ictal and interictal EEG signals (see Fig. 7 (a)). Therefore, post-processing is needed for accurate prediction of epileptic seizure on LS-SVM classified signals. In the post-processing, two-step $u$-of-$v$ analysis is performed to predict an impending seizure by analyzing preictal/ictal and interictal EEG signals where preictal/ictal period represents '1' and interictal period represents '0'. The presence of equal or more than $u$ number of '1' out of $v$

This article has been accepted for publication in a future issue of this journal, but has not been fully edited. Content may change prior to final publication. Citation information: DOI 10.1109/TBME.2016.2553131, IEEE Transactions on Biomedical Engineering

number of consecutive windows (note that a five minute window is used in the experiments), then the prediction horizon is labeled as preictal/ictal period, otherwise, it is labeled as interictal period. In two-step post-processing, 3-of-5 (i.e. $u$ = 3 and $v$ = 5) and 2-of-6 analysis are performed to identify the prediction horizon of the five minute window in total, prior to a seizure. The five minute decision is divided into two steps: the first step consists of 50 seconds i.e. five 10 second epochs; the second step consists of six 50 second windows. In the first step, if at least three epochs have a classified value as '1' then all five epochs are considered '1'. In the second step, six 50 seconds windows are to be considered to make a final decision. If at least two 50 second windows have '1' results then the entire five minute window is regulated as '1' otherwise it is '0'. It is to be noted that in order to prevent the impending seizure by administrating drugs [1], the five minute window is sufficient. Fig. 7(b) shows the seizure prediction result as a decision is taken in each five minute window based on the two-step decision. In each step, different sized windows were investigated; however the proposed two-step method is the best regarding the PA and FPR. Fig. 7 demonstrates the classified results from the LS-SVM and the final decision after regularization. This confirms that regularization is able to remove a number of misclassifications.

## III. SPH AND PREDICTABILITY BY CHANCE

A clinical application of the seizure prediction method is able to generate an alarm of an upcoming seizure and an intervention system can control a seizure. A perfect seizure prediction method has to predict an upcoming seizure by generating an alarm and indicate the exact time of a seizure occurring. It is suggested by Mormann *et al*. [18], Winterhalder *et al.* [17], and Snyder *et al*. [19] to consider *seizure occurrence period* (SOP) which is indicated as the period where seizure is expected. In addition, the *seizure prediction horizon* (SPH) is considered for clinical intervention which is the minimum window of time between the alarm being generated by the prediction method and the beginning of the SOP.

To evaluate the performance of a seizure prediction algorithm, sensitivity over chance level needs to be calculated. The successful and unsuccessful warnings are shown in Fig. 8. The first row of Fig. 8 represents the ideal seizure alarm time, which is expected for the alarm signal to be activated, i.e. the alarm signal should be activated at the starting point of the preictal period and remained active for whole preictal period. The second row of Fig. 8 also represents a successful seizure prediction where preictal classification i.e. alarm, starts late and continues until onset of the actual seizure. The third row of Fig. 8 represents an unsuccessful seizure prediction where the preictal classification does not continue until actual seizure onset. To verify the performance of the proposed prediction method, it is important to measure chance level sensitivity. The chance level sensitivity $S_{nc}$ is defined in [19] as:

$$S_{nc} = 1 - \exp(-\ell_W \mu_W + (1 - e^{\ell_W \mu_{W0}})) \quad (17)$$

where Poisson rate $\ell_W = (1/\mu_W)\ln(1-\eta_W)$.

In (17), $\mu_{W0}$ is the corresponding SPH that is the detection interval, $\mu_W$ is the warning duration that is the sum of SPH, and $\eta_W$ is the proportion of *time under warning* (TUW).

The sensitivity improvement over chance level can be measured by p-value which is defined [19] as

$$\rho = 1 - \theta(\hat{\lambda}_p - 1, \hat{\lambda}_a, S_{nc}) \quad (18)$$

where $\theta$ is the binomial cumulative distribution function, $\hat{\lambda}_p$ is the number of predicted seizures, and $\hat{\lambda}_a$ is the actual seizures.

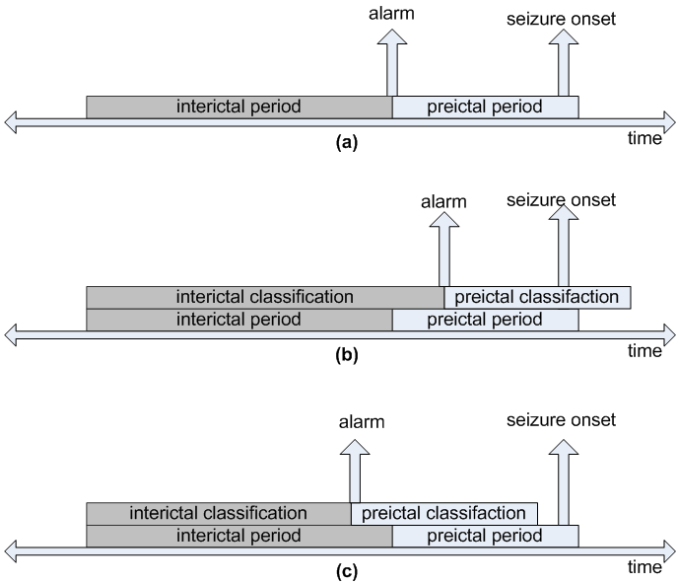


Fig. 8. Seizure prediction horizon (SPH) of the proposed prediction method to predict upcoming seizure by generating an alarm where (a) interictal and preictal periods with ideal alarm time, (b) a successful seizure predictor and (c) a unsuccessful seizure predictor.

## IV. RESULTS AND DISCUSSIONS

The paper proposes a seizure prediction method based on phase correlation and CFD by analyzing EEG signals

This article has been accepted for publication in a future issue of this journal, but has not been fully edited. Content may change prior to final publication. Citation information: DOI 10.1109/TBME.2016.2553131, IEEE Transactions on Biomedical Engineering

from different patients having different brain locations, sex, age, seizure types and electrodes. The EEG signals from different locations of the brain are firstly extracted by an undulated global feature using the customized phase correlation between the reference epoch and current epoch, and undulated local feature using customized CFD of an EEG signal. A classifier then classifies interictal and preictal/ictal signals. A two-step regularization-based decision making strategy is applied to predict the seizure for better PA with low FPR.

PA and FPR are the popular criteria used to evaluate performance of the techniques for prediction of epileptic seizure. Thus they are used in the experiments. The PA is defined in [47] as:

$$\Omega = (\Pi_s / \Pi_a) * 100 \quad (19)$$

$$FPR = Nf / Nt \quad (20)$$

where $\Omega$ is the PA, $\Pi_s$ is the number of correctly predicted seizures, $\Pi_a$ is the total number of seizures, $Nf$ is the number of inaccurately predicted seizures, and $Nt$ is the total time of EEG signals.

Comparisons of the performance of the proposed method with a number of relevant and recent methods [23]-[27] are made. Patients' detailed information from the benchmark data set [29] and the comparison of prediction results of the proposed method with two state-of-the-art methods [24] and [2] are given in Table 1. Some entries in the table for state-of-the-art methods are

TABLE 1. PATIENTS DETAILS AND PREDICTED SEIZURE USING THE PHASE CORRELATION AND PROPOSED METHOD.

| **Patient No.** | **S/A** | **Seizure Type** | **Electrodes** | Brain Location | Total Seizures | **[24]** | | **[2]** | | **Only using UGF** | | **Proposed Method i.e. UGF+ULF** | |
|---|---|---|---|---|---|---|---|---|---|---|---|---|---|
| | | | | | | **PA (%)** | **FA** | **PA (%)** | **FA** | **PA (%)** | **FA** | **PA (%)** | **FA** |
| 1 | F/15 | SP,CP | g, s | Frontal | 4 | 100 | 0 | 100 | 1 | 75.0 | 6 | 100 | 3 |
| 2 | M/38 | SP,CP,GTC | d | Temporal | 3 | - | - | - | - | 67.0 | 12 | 100 | 2 |
| 3 | M/14 | SP,CP | g, s | Frontal | 5 | 100 | 3 | 100 | 1 | 80.0 | 4 | 100 | 2 |
| 4 | F/26 | SP,CP, GTC | d, g, s | Temporal | 5 | - | - | 100 | 1 | 100 | 0 | 100 | 0 |
| 5 | F/16 | SP,CP, GTC | g, s | Frontal | 5 | 100 | 23 | 100 | 21 | 100 | 3 | 100 | 4 |
| 6 | F/31 | CP, GTC | d, g, s | Temporal/ Occipital | 3 | - | - | 100 | 1 | 100 | 1 | 100 | 2 |
| 7 | F/42 | SP,CP, GTC | d | Temporal | 3 | - | - | 100 | 1 | 100 | 0 | 100 | 0 |
| 8 | F/32 | SP,CP | g, s | Frontal | 2 | - | - | - | - | 0.00 | 0 | 50.0 | 2 |
| 9 | M/44 | CP, GTC | g, s | Temporal /Occipital | 5 | 100 | 3 | 100 | 4 | 100 | 3 | 100 | 1 |
| 10 | M/47 | SP,CP, GTC | d | Temporal | 5 | - | - | 100 | 3 | 100 | 10 | 100 | 4 |
| 11 | F/10 | SP,CP, GTC | g, s | Parietal | 4 | 100 | 9 | 75 | 2 | 75.0 | 5 | 75.0 | 1 |
| 12 | F/42 | SP,CP, GTC | d, g, s | Temporal | 4 | - | - | 100 | 1 | 100 | 1 | 100 | 2 |
| 13 | F/22 | SP,CP, GTC | d, s | Temporal/ Occipital | 2 | - | - | - | - | 50.0 | 3 | 50.0 | 1 |
| 14 | F/41 | CP, GTC | d, s | Frontal/ Temporal | 4 | - | - | 75 | 12 | 100 | 4 | 100 | 1 |
| 15 | M/31 | SP,CP, GTC | d, s | Temporal | 4 | - | - | 100 | 4 | 50.0 | 11 | 100 | 2 |
| 16 | F/50 | SP,CP, GTC | d, s | Temporal | 5 | - | - | 90 | 11 | 100 | 17 | 100 | 5 |
| 17 | M/28 | SP,CP, GTC | s | Temporal | 5 | 100 | 10 | 100 | 1 | 100 | 5 | 100 | 2 |
| 18 | F/25 | SP,CP | s | Frontal | 5 | 100 | 17 | 100 | 1 | 40.0 | 7 | 100 | 2 |
| 19 | F/28 | SP,CP, GTC | s | Frontal | 4 | 100 | 25 | 75 | 24 | 75.0 | 20 | 100 | 3 |
| 20 | M/33 | SP,CP, GTC | d, g, s | Temporal /Parietal | 5 | 100 | 0 | 80 | 16 | 100 | 11 | 75.0 | 5 |
| 21 | M/13 | SP,CP | g, s | Temporal | 5 | - | - | 100 | 4 | 80.0 | 10 | 100 | 3 |

S/A=sex/age, SP=simple partial, CP=complex partial, GTC=generalized tonic-conic, d=depth electrode, g=grid electrode, s=strip electrode, PA= prediction accuracy, FA= false alarm, - indicated that the experiment was not available for this patient.

This article has been accepted for publication in a future issue of this journal, but has not been fully edited. Content may change prior to final publication. Citation information: DOI 10.1109/TBME.2016.2553131, IEEE Transactions on Biomedical Engineering

not available as the method in [24] used only 9 patients and the method in [2] used only 18 patients, whereas the proposed method uses all available patients of the data set. Moreover, it is tested the phase correlation feature only and obtained 83.9% PA with FPR is 1.01/h (see Table 1).

The proposed method successfully provides 100% accuracy for 17 patients and the methods in [24] and [2] provide 100% accuracy for 9 and 13 patients respectively. Moreover, the proposed method provides significantly higher FPR than state-of-the-art methods. As Table 1 shows, the proposed method can predict 83 of 87 seizures correctly, with 47 false alarms. Thus, 95.4% average PA with 0.36/h FPR is obtained by the proposed method.

Table 2 shows that the performance of the proposed method in terms of PA and FPR is comparatively better regarding the five existing relevant methods, by combining PA (i.e. 95.4%) and low FPR (i.e. 0.36/h). A proper functioning (i.e. high sensitivity and low false alarms) of the seizure prediction procedure is important to clinically prevent a seizure. Experiments prove that the proposed method achieves low FPR with high sensitivity.

TABLE 2. COMPARISON RESULTS WITH PROPOSED METHOD AND EXITING METHODS.

| Methods | Prediction Accuracy (PA) | FPR (hour) | Total Patients |
|---|---|---|---|
| [23] | 85.0 | 0.03 | 19 |
| [24] | 100 | 0.41 | 9 |
| [25] | 71.0 | 0.00 | 15 |
| [2] | 94.4 | 0.20 | 18 |
| [26] | 75.8 | 0.09 | 21 |
| Proposed Method | 95.4 | 0.36 | 21 |

Table 3 demonstrates the performance of the proposed method against the performance of seizure predictability by chance. The table shows that the proposed method is able to successfully predict 19 of 21 patients above the chance [14]-[16] based on *p*-value.

Table 4 shows the successful and unsuccessful prediction of a seizure per patient. The table also indicates that the mean advanced prediction time with 95.4% performance accuracy for all patients is 22.16 minutes whereas existing literature [27] achieved 96.30% PA between 1 and 6 minutes.

## V. ANALYSIS

### *A.Different Time Epoch*

In the proposed method, a fixed epoch size is employed to extract undulated global and local features of an EEG signal. To find the best epoch size, experiments are conducted using different epoch sizes such as 5 seconds, 10 seconds, and 15 seconds. The 10 seconds epoch is found to be more consistent in terms of decision values of preictal/ictal and interictal signals i.e. the PA and false alarms of the decision values of the 10 seconds window during preictal/ictal and interictal signals are the minimum compared to the decision values for a 5 or 15 seconds-epoch (shown in Fig. 9). Therefore, a 10 seconds epoch is applied in the experiments.

TABLE 3. CALCULATED SENSITIVITY BY PROPOSED METHOD AND CHANCE LEVEL.

| PN | TS | Sensitivity by proposed method (%) | Proportion of time in warning $\eta_W$ (%) | *p*-value |
|---|---|---|---|---|
| 1 | 4 | 100 | 20.8 | 0.000005 |
| 2 | 3 | 100 | 22.2 | 0.000133 |
| 3 | 5 | 100 | 23.3 | 0.000000 |
| 4 | 5 | 100 | 32.2 | 0.000003 |
| 5 | 5 | 100 | 27.7 | 0.000001 |
| 6 | 3 | 100 | 27.7 | 0.000280 |
| 7 | 3 | 100 | 33.3 | 0.000532 |
| 8 | 2 | 50 | 12.5 | 0.054148 |
| 9 | 5 | 100 | 33.3 | 0.000003 |
| 10 | 5 | 100 | 25.5 | 0.000001 |
| 11 | 4 | 75 | 25.0 | 0.000756 |
| 12 | 4 | 100 | 26.4 | 0.000015 |
| 13 | 2 | 50 | 18.8 | 0.083184 |
| 14 | 4 | 100 | 33.3 | 0.000043 |
| 15 | 4 | 100 | 23.6 | 0.000009 |
| 16 | 5 | 100 | 27.7 | 0.000001 |
| 17 | 5 | 100 | 32.2 | 0.000003 |
| 18 | 5 | 100 | 24.4 | 0.000001 |
| 19 | 4 | 100 | 26.3 | 0.000014 |
| 20 | 5 | 75 | 8.9 | 0.000001 |
| 21 | 5 | 100 | 23.3 | 0.000000 |
| PN= Patient Number, TS=Total Seizures | | | | |

### *B.Different Sample Shift Justification*

In the proposed method, 128 sample-shift is used for each epoch to extract ULF in Equation (11) & (12) (detail of the 128 shifted sample size is described in Section II. C). The performance of the ULF is investigated using a different sample shift (i.e. 64, 128 and 256 sample) for each shifting epoch. For the investigation, EEG signals from different patients with different brain locations are used. It is to be noted that, 128 shifted window carries good PA compared to the 64 and 256 sample shift (see Table 5).

This article has been accepted for publication in a future issue of this journal, but has not been fully edited. Content may change prior to final publication. Citation information: DOI 10.1109/TBME.2016.2553131, IEEE Transactions on Biomedical Engineering

TABLE 4. CALCULATED EARLY PREDICTION TIME PER SEIZURE AND PER PATIENT AND ITS MEAN VALUE USING PROPOSED METHOD.

| PN | TS | Predicting a seizure onset in terms of minutes | | | | | |
|---|---|---|---|---|---|---|---|
| | | SZ 1 | SZ 2 | SZ 3 | SZ 4 | SZ 5 | Average |
| 1 | 4 | 8 | 23 | 9 | 30 | - | 17.50 |
| 2 | 3 | 6 | 22 | 30 | - | - | 19.33 |
| 3 | 5 | 3 | 30 | 4 | 30 | 30 | 19.40 |
| 4 | 5 | 30 | 30 | 24 | 30 | 30 | 28.80 |
| 5 | 5 | 30 | 5 | 30 | 30 | 30 | 25.00 |
| 6 | 3 | 30 | 30 | 14 | - | - | 24.67 |
| 7 | 3 | 30 | 30 | 30 | - | - | 30.00 |
| 8 | 2 | 7 | 0 | - | - | - | 3.50 |
| 9 | 5 | 30 | 30 | 30 | 30 | 30 | 30.00 |
| 10 | 5 | 8 | 26 | 30 | 30 | 26 | 24.00 |
| 11 | 4 | 0 | 30 | 30 | 30 | - | 22.5 |
| 12 | 4 | 25 | 30 | 30 | 7 | - | 23.00 |
| 13 | 2 | 30 | 0 | - | - | - | 15.00 |
| 14 | 4 | 30 | 30 | 30 | 30 | - | 30.00 |
| 15 | 4 | 25 | 6 | 27 | 30 | - | 22.00 |
| 16 | 5 | 5 | 30 | 30 | 30 | 30 | 25.80 |
| 17 | 5 | 30 | 30 | 30 | 27 | 30 | 29.40 |
| 18 | 5 | 30 | 30 | 11 | 29 | 10 | 22.00 |
| 19 | 4 | 6 | 30 | 30 | 30 | - | 24.00 |
| 20 | 5 | 15 | 11 | 0 | 6 | 7 | 7.80 |
| 21 | 5 | 30 | 30 | 12 | 6 | 30 | 21.60 |
| **Average early prediction time: 22.16 minutes** | | | | | | | |

SZ=seizure, PN=patient number, TS=total seizures, - indicated that seizure is not available for this patient.

TABLE 5. COMPARISON RESULTS AMONG 64, 128, AND 256 SHIFT ANALYSIS USING UNDULATED LOCAL FEATURE EXTRACTION TECHNIQUE FOR DIFFERENT PATIENTS WITH DIFFERENT BRAIN LOCATIONS.

| PN | Brain Location (Lobe) | TS | Predicted Seizures | | | PA (%) | | |
|---|---|---|---|---|---|---|---|---|
| | | | 64 | 128 | 256 | 64 | 128 | 256 |
| 4 | Temporal | 5 | 5 | 5 | 4 | 100 | 100 | 80 |
| 13 | Temporal/ Occipital | 2 | 1 | 2 | 2 | 50 | 100 | 100 |
| 18 | Frontal | 5 | 4 | 5 | 4 | 80 | 100 | 80 |
| 19 | Frontal | 4 | 3 | 4 | 4 | 75 | 100 | 100 |
| **PN= Patient Number, TS= Total Seizure, PA=Prediction Accuracy** | | | | | | | | |

## VI. CONCLUSION

In this paper an epileptic seizure prediction method is proposed which exploits undulated global and local features together with a regularization technique to successfully and unsuccessfully predict the seizure onset. The global feature is extracted using the phase correlation between two consecutive epochs of an EEG signal and the local feature is extracted using a weighted cost function comprising fluctuation and deviation

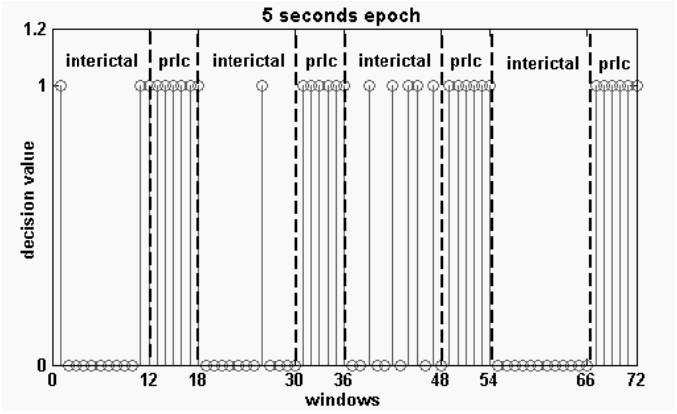


(a) Decision on classified values using 5 seconds epoch of interictal and preictal/ictal (i.e. prIc) periods.

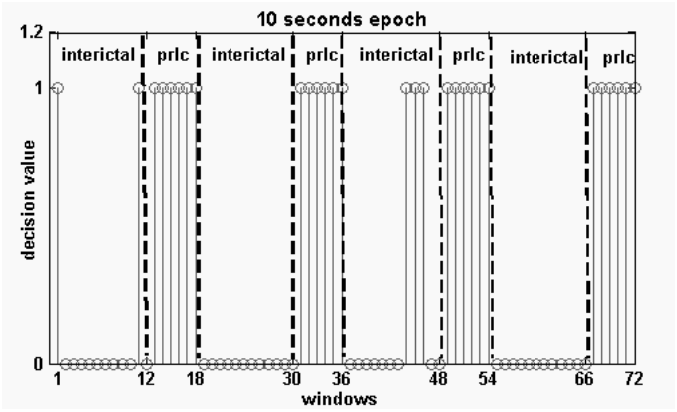


(b) Decision on classified values using 10 seconds epoch of interictal and preictal/ictal (i.e. prIc) periods.

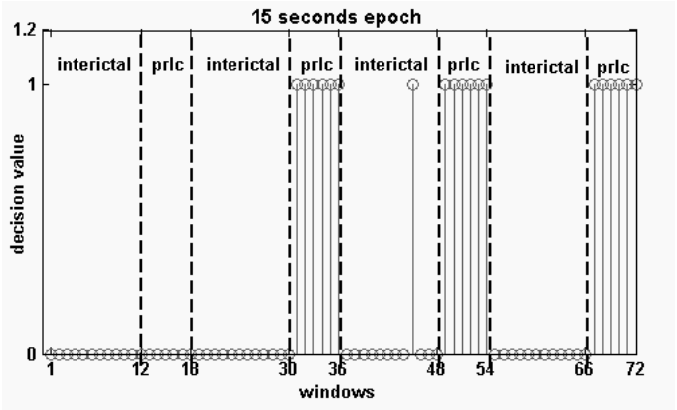


(c) Decision on classified values using 15 seconds epoch of interictal and preictal/ictal (i.e. prIc) periods.

Fig. 9. Decision for seizure prediction using Patient 11 data set. The decision values of preictal/ictal (i.e. prIc) and interictal EEG signals using different window sizes where (a), (b), and (c) represent the 5 second, 10 second, and 15 second window, respectively.

within an epoch. The popular LS-SVM classifier is used to classify the interictal, preictal, and ictal signals. To purify the classified output, a two-step post-processing regularization technique is also applied for the final output. The experimental results are obvious in that the

proposed prediction method provides high prediction accuracy (95.4%) and low FPR (i.e. 0.36/h) for all patients from a challenging benchmark data set, without any explicit artifacts removal technique. The statistical analysis confirms that the proposed method is able to predict seizures in 19 of 21 patients from a benchmark data set above the chance level. Moreover, the proposed method outperforms six existing relevant state-of-the-art methods considering the balance between the PA and FPR.

Freiburg data set is the benchmark resource in modern seizure prediction approaches that contains widely varieties of seizures and patients. The data set has continuous data within interictal or preictal EEG signals, however, there is no clear chronological order between interictal and preictal signals. Due to the lack of publicly available data set, it is not possible to test the performance of the proposed technique against other relevant techniques using true continuous data. This is a retrospective study and thus that prospective testing with continuous long lasting data is needed to validate the reported results. In this regard, we are planning in future to test the proposed algorithm for a true continuous data set.

## REFERENCES


[1] S. Santaniello, *et al*. (2011, Dec). Quickest detection of drug-resistant seizures: An optimal control approach. *Epilepsy & Behavior*, 22(2011), pp. S49-S60.

[2] Y. Park, *et al*. (2011, Oct). Seizure prediction with spectral power of EEG using cost-sensitive support vector machines. *Epilepsia*, 52(10), pp. 1761-1770.

[3] Y. Tang and D.M. Durand. (2012, Mar). A tunable support vector machine assembly classifier for epileptic seizure detection. *Expert Systems with Applications*, 39 (4), pp. 3925–3938.

[4] M. Guttinger, *et al*. (2005, May). Seizure suppression and lack of adenosine A1 receptor desensitization after focal long-term delivery of adenosine by encapsulated myoblasts. *Experimental Neurology*, 193(1), pp. 53–64.

[5] O. A. Rosso, *et al*. (2003, June). Wavelet analysis of generalized tonic-clonic epileptic seizures. *Signal Processing*, 83 (6), pp. 1275–1289.

[6] V. L. Dorr, *et al*. (2007, July). Extraction of reproducible seizure patterns based on EEG scalp correlations. *Biomedical Signal Processing and Control*, 2(3), pp. 154–162.

[7] F. H. Lopes da Silva. (2008). The impact of EEG/MEG signal processing and modeling in the diagnostic and management of epilepsy. *IEEE Reviews in Biomedical Engineering*, 1, pp. 143–156.

[8] M. Z. Parvez and M. Paul. (2014, Dec). Epileptic seizure detection by analyzing EEG signals using different transformation techniques. *Neurocomputing*, 145, pp. 190-200.

[9] M. J. Cook, *et al*. (2013). Prediction of seizure likelihood with a long-term, implanted seizure advisory system in patients with drug-resistant epilepsy: a first-in-man study. *The Lancet Neurology*, 12, pp. 563-571.

[10] M. Le Van Quyen, *et al*. (2001). Anticipation of epileptic seizures from standard EEG recordings. *The Lancet*, 357, pp. 183-188.

[11] F. Mormann, *et al*. (2003). Epileptic seizures are preceded by a decrease in synchronization. *Epilepsy Research*, 53, pp. 173-185.

[12] L. D. Iasemidis, *et al*. (2003). Adaptive epileptic seizure prediction system. IEEE Transactions on Biomedical Engineering, 50, pp. 616-627.

[13] K. Lehnertz and C. E. Elger. (1998). Can Epileptic Seizures be Predicted? Evidence from Nonlinear Time Series Analysis of Brain Electrical Activity. *Physical Review Letters*, 80, pp. 5019-5022.

[14] K. Gadhoumi, *et al*. (2013). Seizure prediction in patients with mesial temporal lobe epilepsy using EEG measures of state similarity. *Clinical Neurophysiology*, 124, pp. 1745-1754.

[15] K. Gadhoumi, *et al*. (2015). Seizure prediction for therapeutic devices: A review. *Journal of Neuroscience Methods*.

[16] K. Gadhoumi, *et al*. (2015). Scale Invariance Properties of Intracerebral EEG Improve Seizure Prediction in Mesial Temporal Lobe Epilepsy. *PLoS ONE*, 10, p. e0121182.

[17] M. Winterhalder, *et al*. (2003). The seizure prediction characteristic: a general framework to assess and compare seizure prediction methods. *Epilepsy & Behavior*, 4, pp. 318-325.

[18] F. Mormann, *et al*. (2007). Seizure prediction: the long and winding road. *Brain*, 130(2), pp. 314-333.

[19] D. E. Snyder, *et al*. (2008). The Statistics of a Practical Seizure Warning System. *Journal of Neural Engineering*, 5(4), pp. 392-401.

[20] A. Aarabi and B. He. (2014). Seizure prediction in hippocampal and neocortical epilepsy using a model-based approach. *Clinical Neurophysiology*, 125(5), pp. 930-940.

[21] K. A. Davis, *et al*. (2016). Mining continuous intracranial EEG in focal canine epilepsy: Relating interictal bursts to seizure onsets. *Epilepsia*, 57(1), pp. 89-98.

[22] L. Yunfeng, *et al*. (2014). Noninvasive Imaging of the High Frequency Brain Activity in Focal Epilepsy Patients. *IEEE Transactions on Biomedical Engineering*, 61(6), pp. 1660-1667.

[23] J.R. Williamson, *et al*. (2012, Oct). Seizure prediction using EEG spatiotemporal correlation structure. *Epilepsy & Behavior*, 25 (2), pp. 230–238.

[24] L. Chisci, *et al*. (2010, May). Real-Time Epileptic Seizure Prediction Using AR Models and Support Vector Machines. *IEEE Transactions on Biomedical Engineering*, 57(5), pp. 1124-1132.

[25] P. Mirowski, *et al*. (2009, Nov). Classification of patterns of EEG synchronization for seizure prediction. *Clinical Neurophysiology*, 120(11), pp. 1927-1940.

[26] S. Li, *et al*. (2013, Oct). Seizure Prediction Using Spike Rate of Intracranial EEG. *IEEE Transactions on Neural Systems and Rehabilitation Engineering*, 21(6), pp. 880-886.

[27] N. Moghim and D. W. Corne. (2014, Jun). Predicting Epileptic Seizures in Advance. *PLoS ONE*, 9(6), e99334.

[28] J. Rasekhi, *et al*. (2013). Preprocessing effects of 22 linear univariate features on the performance of seizure prediction methods. *Journal of Neuroscience Methods*, 217, pp. 9–16.

[29] EEG Data Set: Epilepsy Center of the University Hospital of Freiburg. (2012, June 10). Available: http://epilepsy.uni-freiburg.de/freiburg-seizure-prediction-project/eeg-database.

[30] L. Ding, *et al*. (2009). Three-dimensional Imaging of Complex Neural Activation in Humans from EEG. *IEEE Transactions on Biomedical Engineering*, 56(8), pp.1980–1988.

[31] M. Paul, *et al*. (2011). Direct Intermode Selection for H.264 Video Coding Using Phase Correlation. *IEEE Transactions on Image Processing*, 20(2), pp. 461-473.

[32] Y. Xie, *et al*. (2014, Jan). A physics-based defects model and inspection algorithm for automatic visual inspection. *Optics and Lasers in Engineering*, 52 (2014), pp. 218-223.

[33] M. Z. Parvez and M. Paul. (2015, Feb). Epileptic seizure detection by exploiting temporal correlation of electroencephalogram signals. *IET Signal Processing*, 9(6), pp. 467–475.

[34] V. Bajaj and R.B. Pachori. (2013, Mar). Epileptic seizure detection based on the instantaneous area of analytic intrinsic mode functions of

[35] EEG signals. *Biomedical Engineering Letters*, 3(1), pp. 17-21.

[36] W. Zhou, *et al*. (2013, Apr). Epileptic Seizure Detection Using Lacunarity and Bayesian Linear Discriminant Analysis in Intracranial EEG. *IEEE Transactions on Biomedical Engineering*, 60(12), pp. 3375-3381.

[37] M. Paul, *et al*. (2014, Oct). A Long Term Reference Frame for Hierarchical B-Picture based Video Coding. *IEEE Transactions on Circuits and Systems for Video Technology*, 24 (10), pp. 1729-1742.

[38] S. Abe, Support vector machine for pattern classification, Springer, 2010.

[39] S. Mihandoost, *et al*. (2012). Automatic feature extraction using generalised autoregressive conditional heteroscedasticity model: an application to electroencephalogram classification. *IET Signal Processing*, 6(9), pp. 829-838.

[40] R. B. Pachori and V. Bajaj. (2011, Dec). Analysis of normal and epileptic seizure EEG signals using empirical mode decomposition. *Computer Methods and Programs in Biomedicine*, 104(3), pp. 373-381.

[41] H. Wang and D. Hu," Comparison of SVM and LS-SVM for Regression," *International Conference on Neural Networks and Brain*, 2005, 1, pp. 279 – 283.
[42] K. D. Brabanter, *et al*., " LS-SVM Lab Toolbox User's Guide, version 1.8, Katholieke Universiteit Leuven", 2011.
[43] J. A. K. Suykens and J. Vandewalle. (1999). Least Squares Support Vector Machine Classifiers. *Neural Processing Letters*, 9(3), pp. 293–300.
[44] V. Bajaj and R. B. Pachori. (2012).Classification of Seizure and Non-seizure EEG Signals using Empirical Mode Decomposition. *IEEE Transactions on Information Technology in Biomedicine*, 16(6), pp. 1135-1142.
[45] M. Paul, *et al*. (2009). An Efficient Mode Selection Prior to the Actual Encoding for H.264/AVC Encoder. *IEEE Transactions on Multimedia*, 11(4), pp.581-588.
[46] H. Xing, *et al*. (2009). Linear feature- weighted support vector machine. *Fuzzy Information and Engineering*, Springer, 1(3), pp. 289-305.
[47] Z. Zhang, *et al*. (2014, Oct). Construction of rules for seizure prediction based on approximate entropy. *Clinical Neurophysiology*, 125(10), pp. 1959–1966.